Inorg. Chem. **2007**, *46*, 5691–5699

Conformational Effect of 2,6-Bis(imidazol-1-yl)pyridine on the Self-Assembly of 1D Coordination Chains: Spontaneous Resolution, Supramolecular Isomerism, and Structural Transformation

Chih-Yuan Chen, Pi-Yun Cheng, Hsin-Hsuan Wu, and Hon Man Lee*

Department of Chemistry, National Changhua University of Education, Changhua 50058, Taiwan

Received March 6, 2007

The achiral 2,6-bis(imidazol-1-yl)pyridine (L) was used as the ditopic organic tecton for the formation of coordination polymers with Zn(II) ions. Hydrothermal reaction between L and ZnX_2 (X = Br, Cl) afforded spontaneous resolved double helical motifs in $ZnLCl_2 \cdot 0.5H_2O$ (**1**) and $ZnLBr_2 \cdot 0.25H_2O$ (**2**). In the homochiral crystals of **1a** and **2a**, the helices are of *M*-helicity, whereas, in **1b** and **2b**, they are of *P*-helicity. In contrast, solvothermal reaction between L and $ZnCl_2$ in dried DMF afforded achiral $ZnLCl_2$ (**3a**), which exhibits a zigzag polymeric motif. An achiral polymorph **3b** which contains 2_1 helical chains was obtained in wet DMF. The formation of different 1D motifs was related to the conformations of L. All these compounds were characterized by infrared spectroscopy, elemental analyses, and single-crystal X-ray diffraction. As revealed by thermal gravimetric analysis and powder X-ray diffraction study, the homochiral motif in **1** was stable even upon removal of guest water molecules. Contrastingly, structural transformation from **3a** or **3b** to **1** is possible upon hydration.

Introduction

The design and preparation of helical coordination polymers are of intense interests because of their potential applications in the fields of asymmetric catalysis, enantiomer separation, chiral synthesis, and nonlinear optics.[1,2] The intriguing property of helical coordination polymer is its chirality. A reliable strategy to obtain homochiral helical coordination polymers is by using enantiopure ditopic organic tectons. To date, various examples of homochiral polymeric materials obtained by such methodology have been published.[3] On the other hand, increasing amount of efforts have been devoted to assemble homochiral helical coordination polymers with achiral building blocks by spontaneous resolution.[4] Although the detailed mechanism is not clear, it has been shown that crystals grew from a single nucleation site that is homochiral.[5,6] In any given batch, generally, multinucleation sites will lead to the formation of a conglomerate, which is a mechanical mixture of homochiral crystals of opposite helicities (*M*- and *P*-helices).[7−16] Achiral ditopic ligands of diverse structural characteristics (rigid

* To whom correspondence should be addressed. E-mail: leehm@cc.ncue.edu.tw. Phone: +886 4 7232105 ext. 3523. Fax: +886 4 7211190.

(1) Janiak, C. *Dalton Trans.* **2003**, 2781 and references therein.
(2) Kesanli, B.; Lin, W. *Coord. Chem. Rev.* **2003**, *246*, 305 and references therein.
(3) See for examples: (a) Wu, B.; Zhang, W.-J.; Yu, S.-Y.; Wu, X.-T. *J. Chem. Soc., Dalton Trans*. **1997**, 1795. (b) Bowyer, P. K.; Porter, K. A.; Rae, A. D.; Willis, A. C.; Wild, S. B. *Chem. Commun*. **1998**, 1153. (c) Mamula, O.; von Zelewsky, A.; Bark, T.; Bernardinelli, G. *Angew. Chem., Int. Ed*. **1999**, *38*, 2945. (d) Cutland-Van Noord, A. D.; Kampf, J. W.; Pecoraro, V. L. *Angew. Chem., Int. Ed*. **2002**, *41*, 4667. (e) Grosshans, P.; Jouaiti, A.; Bulach, V.; Planeix, J.-M.; Hosseini, M. W.; Nicoud, J.-F. *Chem. Commun*. **2003**, 1336. (f) Anthony, S. P.; Radhakrishnan, T. P. *Chem. Commun*. **2004**, 1058. (g) Anokhina, E. V.; Jacobson, A. J. *J. Am. Chem. Soc*. **2004**, *126*, 3044. (h) Roth, A.; Koth, D.; Gottshaldt, M.; Plass, W. *Cryst. Growth Des*. **2006**, *6*, 2655.
(4) Han, L.; Hong, M. *Inorg. Chem. Commun*. **2005**, *8*, 406 and references therein.
(5) Ezuhara, T.; Endo, K.; Aoyama, Y. *J. Am. Chem. Soc*. **1999**, *121*, 3279.
(6) Tian, G.; Zhu, G.; Yang, X.; Fang, Q.; Xue, M.; Sun, J.; Wei, Y.; Qiu, S. *Chem. Commun*. **2005**, 1396.
(7) Biradha, K.; Seward, C.; Zaworotko, M. J. *Angew. Chem., Int. Ed*. **1999**, *38*, 492.
(8) Tabellion, F. M.; Seidel, S. R.; Arif, A. M.; Stang, P. J. *Angew. Chem., Int. Ed*. **2001**, *40*, 1529.
(9) Sasa, M.; Tanaka, K.; Bu, X.−H.; Shiro, M.; Shionoya, M. *J. Am. Chem. Soc*. **2001**, *123*, 10750.
(10) Siemeling, U.; Scheppelmann, I.; Neumann, B.; Stammler, A.; Stammler, H.-G.; Frelek, J. *Chem. Commun*. **2003**, 2236.
(11) Gao, E.-Q.; Yue, Y.-F.; Bai, S.-Q.; He, Z.; Yan, C.-H. *J. Am. Chem. Soc*. **2004**, *126*, 1419.
(12) Chen, X. D.; Du, M.; Mark, T. C. W. *Chem. Commun*. **2005**, 4417.
(13) Li, F.; Li, T.; Li, X.; Li, X.; Wang, Y.; Cao, R. *Cryst. Growth Des*. **2006**, *6*, 1458.
(14) Sun, Q.; Bai, Y.; He, G.; Duan, C.; Lin, Z.; Meng, Q. *Chem. Commun*. **2006**, 2777.
(15) Balamurugan, V.; Mukherjee, R. *Inorg. Chim. Acta* **2006**, *359*, 1376.
(16) Gu, X.; Xue, D. *Inorg. Chem*. **2006**, *45*, 9257.

10.1021/ic700428e CCC: $37.00 © 2007 American Chemical Society
Published on Web 06/15/2007

Scheme 1. Different Possible Conformations of L and Its Reaction with Zinc(II) Halides

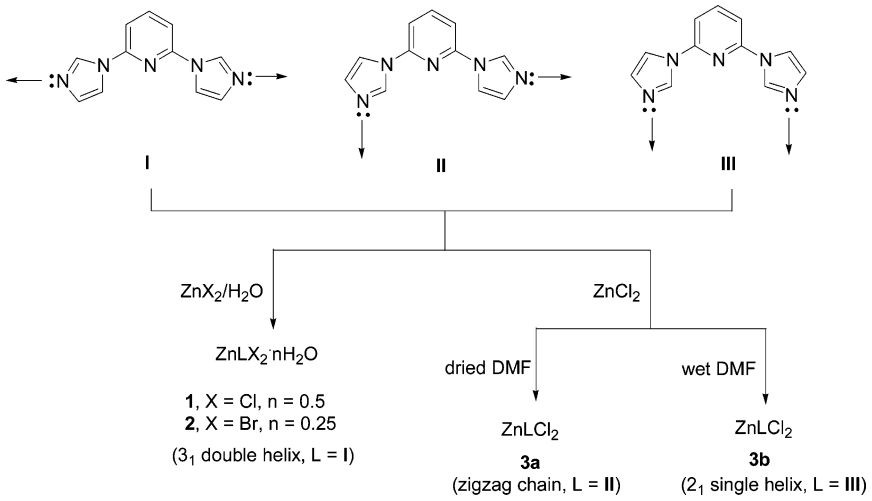

flexible asymmetric) have been employed as the organic tectons Ni(II),[7,17] Cu(II),[17] Cu(I),[18] Ag(I),[12,14,16] Zn(II),[9,10,19−21] Cd(II),[5,13,15,20,21−23] and Hg(II).[10]

Lately, we explored the possibility of employing the achiral, 2,6-bis(imidazol-1-yl)pyridine (L) as the ditopic organic tecton for the self-assembly of helical Zn(II) coordination polymers. Our interest in L is based on the fact that it is a hingelike molecule.[4] The three heterocyclic rings are rigid but connected by two rotatable C−N bonds (Scheme 1). The different conformers arise from the flexibility can be interpreted by the arrangements of metal ions and guest molecules for the formation of diverse supramolecular structures.[18] In addition, it contains a central pyridyl ring, which is anticipated to be nonmetal binding but allows strong $\pi-\pi$ stacking interactions for the stabilization of solid-state structures. Herein, we report our successful effort in combining of L and ZnX_2 (X = Cl, Br) under different reaction conditions to afford a variety of 1D coordination motifs, including spontaneous resolved $3_1(3_2)$ double helix, 2_1 single helix, and zigzag chains. The formation of $3_1(3_2)$ double helical structure is apparently controlled by the hydrogen-bonding interactions involving the guest water molecules. In DMF, genuine supramolecular isomers (polymorphs) of 2_1 single helix and zigzag chain are obtained. The homochiral motif of double helix was retained upon removal of guest water molecules, whereas structural transformation from the guest-free motifs to the homochiral motif is possible upon hydration.

Experimental Section

Materials and General Methods. All reactions were performed under a dry nitrogen atmosphere using standard Schlenk technique. All solvents used were purified according to standard procedures.[24] Commercially available chemicals were purchased from Aldrich or Acros. ^{1}H and ^{13}C{^{1}H} NMR spectra were recorded at 300.13 and 75.48 MHz, respectively, on a Bruker AV-300 spectrometer. Chemical shifts for ^{1}H and ^{13}C spectra were recorded in ppm relative to residual proton of $CDCl_3$ (^{1}H, δ 7.24; ^{13}C, δ 77.0) and CD_2Cl_2 (^{1}H, δ 5.32; ^{13}C, δ 53.8). Elemental analyses were performed on a Heraeus CHN-OS Rapid Elemental Analyzer at the Instruments Center of National Chung Hsing University, Chung Hsing, Taiwan. Thermogravimetric analysis (TGA) was performed on a Perkin-Elmer Pyris 6 TGA thermogravimetric analyzer under flowing N_2 gas (40 mL/min), and the heating rate was 20 °C/min. Powder X-ray diffraction (PXRD) measurements were recorded on Shimadzu Lab-X XRD-6000 diffractometers with either Fe Kα, λ = 1.937 28 Å, or Cu Kα, λ = 1.540 60 Å. The synthesis of 2,6-bis(imidazol-1-yl)pyridine (L) was previously described,[25,26] but herein we prepared it with a different procedure.

Synthesis of L. A mixture of 1*H*-imidazole (2.20 g, 33.77 mmol), 2,6-dibromopyridine (2.00 g, 8.44 mmol), KOH (2.85 g, 50.73 mmol), and tetrabutylammonium bromide (0.30 g, 0.93 mmol) in 30 mL of THF was heated under reflux for 2 d. The solvent was then pumped dried under vacuum. The residue was washed with water and extracted twice with dichloromethane. After removal of the solvent, the crude product was purified by flash chromatography on silica gel (10:1 ethyl acetate−methanol) affording the pure product, which was dried under vacuum overnight. Yield: 1.78 g, 74%. NMR and analytical data were same as those reported in the literature.[25,26] IR (KBr/pellet cm^{-1}): 3210 (w), 3101 (ms), 1696 (ms), 1609 (vs), 1493 (vs), 1287 (vs), 1259 (vs), 1174 (ms), 1105 (ms), 1055 (vs), 1007 (vs), 909 (ms), 831 (ms), 809 (ms), 735 (vs), 647 (ms), 604 (w) cm^{-1}. Crystals suitable for structural analysis were obtained by slow evaporation from an acetone solution containing L.

Synthesis of $ZnLCl_2 \cdot 0.5H_2O$ (1). A mixture of anhydrous $ZnCl_2$ (0.19 g, 1.42 mmol) and L (0.20 g, 0.95 mmol) in deionized water

(17) Zang, S.; Su, Y.; Li, Y.; Zhu, H.; Meng, Q. *Inorg. Chem.* **2006**, *45*, 2972.
(18) Zhang, J.-P.; Lin, Y.-Y.; Huang, X.-C.; Chen, X.-M. *Chem. Commun.* **2005**, 1258.
(19) Kondo, M.; Miyazawa, M.; Irie, Y.; Shinagawa, R.; Horiba, T.; Nakamura, A.; Naito, T.; Maeda, K.; Utsuno, S.; Uchida, F. *Chem. Commun.* **2002**, 2156.
(20) Zang, S.; Su, Y.; Li, Y.; Ni, Z.; Meng, Q. *Inorg. Chem.* **2006**, *45*, 174.
(21) Yi, L.; Yang, X.; Lu, T.; Cheng, P. *Cryst. Growth Des.* **2005**, *5*, 1215.
(22) Wang, Y.-T.; Tong, M.-L.; Fan, H.-H.; Wang, H.-Z.; Chen, X.-M. *Dalton Trans.* **2005**, 424.
(23) Zang, S.; Su, Y.; Li, Y.; Ni, Z.; Zhu, H.; Meng, Q. *Inorg. Chem.* **2006**, *45*, 3855.
(24) Armarego, W. L. F.; Chai, C. L. L. *Purification of Laboratory Chemicals*, 5th Ed.; Elsevier Science: Burlington, MA, 2003.
(25) Turnbull, M. M.; Glynn, C. W. *Inorg. Chim. Acta* **2002**, *332*, 92.
(26) Caballero, A.; Díez-Barra, E.; Jalón, F. A.; Merino, S.; Tejed, J. *J. Organomet. Chem.* **2001**, *617−618*, 395.

Table 1. Crystallographic Data for L and **1**−**3**

param	L·H_2O	**1a**	**1b**	**2a**	**2b**	**3a**	**3b**
empirical formula	$C_{11}H_9N_5·H_2O$	$C_{11}H_9Cl_2N_5Zn·0.5H_2O$	$C_{11}H_9Cl_2N_5Zn·0.5H_2O$	$C_{11}H_9Br_2N_5Zn·0.25H_2O$	$C_{11}H_9Br_2N_5Zn·0.25H_2O$	$C_{11}H_9Cl_2N_5Zn$	$C_{11}H_9Cl_2N_5Zn$
fw	229.25	356.53	356.53	440.92	440.92	347.50	347.50
cryst system	monoclinic	trigonal	trigonal	trigonal	trigonal	monoclinic	orthorhombic
space group	$P2_1/c$	$P3_221$	$P3_121$	$P3_221$	$P3_121$	$P2_1/n$	$Pbca$
a, Å	3.7728(6)	9.6116(1)	9.6165(1)	9.7240(5)	9.72760(10)	9.0895(9)	9.4515(5)
b, Å	15.486(3)	9.6116(1)	9.6165(1)	9.7240(5)	9.72760(10)	9.9518(10)	14.2276(8)
c, Å	18.834(3)	25.2776(6)	25.2979(4)	25.710(3)	25.7448(5)	15.1892(15)	20.1329(11)
α, deg	90	90	90	90	90	90	90
β, deg	95.665(5)	90	90	90	90	98.945(2)	90
γ, deg	90	120	120	120	120	90	90
V, Å^3	1095.1(3)	2022.36(6)	2026.04(4)	2105.4(3)	2109.75(5)	1357.3(2)	2707.3(3)
T, K	*150(2)*	*150(2)*	*150(2)*	*150(2)*	*150(2)*	*150(2)*	*150(2)*
Z	4	6	6	6	6	4	8
D_c (g cm^{-3})	1.391	1.751	1.748	2.084	2.080	1.701	1.705
no. of unique data	2856	3452	3463	3583	3614	3485	3484
no. of params refined	191	177	177	177	177	172	172
R_1[a] [$I > 2\sigma I$]	0.0488	0.0267	0.0229	0.0197	0.0250	0.0203	0.0222
wR_2[b] (all data)	0.1375	0.0714	0.0631	0.0475	0.0494	0.0542	0.0611
Flack param	n/a	−0.004(11)	0.002(10)	0.007(8)	0.015(9)	n/a	n/a

[a] $R_1 = \sum(||F_o| - |F_c||)/\sum|F_o|$. [b] $wR_2 = [\sum(|F_o|^2 - |F_c|^2)^2/\sum(F_o^2)]^{1/2}$.

(20 mL) was placed in a 50 mL Teflon-lined autoclave, which was heated according to the following temperature program: heated to 140 °C in 50 min; maintained at this temperature for 5 h; cooled to 110 °C in 30 min‘ maintained at this temperature for 3 h; cooled to 90 °C in 20 min; maintained at this temperature for 4 h; then allowed to cool to RT (room temperature) slowly. The colorless crystals were filtered under suction, washed with water, and dried in air. Yield: 0.23 g, 66%. Anal. Calcd for $C_{11}H_9Cl_2N_5Zn·0.5H_2O$: C, 37.06; H, 2.83; N, 19.64. Found: C, 37.05; H, 2.80; N, 19.70. Mp: 387 °C. IR (KBr/pellet, cm^{-1}): 3527 (w), 3132 (ms), 1610 (vs), 1507 (vs), 1466 (vs), 1303 (vs), 1277 (vs), 1171 (ms), 1101 (ms), 1071 (ms), 1010 (ms), 942 (ms), 848 (ms), 794 (ms), 765 (vs), 724 (ms), 644 (vs), 531 (ms) cm^{-1}.

Synthesis of $ZnLBr_2·0.25H_2O$ (2). This compound was prepared by following a procedure similar to that for **1**. Anhydrous $ZnBr_2$ (0.10 g, 0.47 mmol) and L (0.10 g, 0.47 mmol) were used. Colorless crystals were obtained. Yield: 0.19 g, 88%. Anal. Calcd for $C_{11}H_9Br_2N_5Zn·0.25H_2O$: C, 29.93; H, 2.17; N, 15.88. Found: C, 29.82; H, 2.13; N, 15.81. Mp: 395 °C. IR (KBr/pellet, cm^{-1}): 3537 (w), 3116 (ms), 1606 (vs), 1504 (vs), 1462 (vs), 1302 (vs), 1273 (vs), 1167 (ms), 1101 (ms), 1068 (ms), 1009 (ms), 942 (ms), 837 (ms), 794 (ms), 763 (vs), 642 (vs), 497 (ms).

Synthesis of $ZnLCl_2$ (3). A sample $ZnCl_2$ (0.20 g, 1.46 mmol) was weighted in a glovebox and placed into a 20-mL scintillation vial. To the vial was added L (0.20 g, 0.95 mmol) and dried DMF (10 mL). The mixture was allowed to heat at 140 °C in an oil bath for 30 h. After cooling to RT, the colorless crystals was filtered and washed with several times with acetone. The solid is pure polymorph **3a** according to single-crystal X-ray and PXRD studies. Yield: 0.18 g, 55%. Anal. Calcd for $C_{11}H_9Cl_2N_5Zn$: C, 38.02; H, 2.61; N, 20.15. Found: C, 38.12; H, 2.63; N, 20.04. Mp: 382 °C. IR (KBr/pellet, cm^{-1}): 3114 (ms), 1609 (vs), 1500 (vs), 1466 (vs), 1311 (vs), 1268 (vs), 1233 (vs), 1179 (ms), 1112 (ms), 1067 (vs), 1008 (ms), 941 (ms), 851 (ms), 794 (vs), 756 (vs), 646 (vs), 497 (ms). A similar reaction in wet DMF afforded colorless crystals, which consist of **1** and polymorph **3b** according to single-crystal X-ray and PXRD analyses. Mp of **3b**: 381 °C (from a single crystal of **3b**).

Structural Transformation from 3 to 1. Crystals of **3a** was allowed to stir in water at 50 °C overnight. The amorphous powder remained was filtered and dried under suction. The solid was analyzed by PXRD study. Similarly, the mixture of **1** and **3b** was allowed to stir in water at room temperature. The amorphous solid was then analyzed by PXRD study.

Table 2. Selected Bond Lengths (Å) and Angles (deg) for L, **1a**, and **2a**

	Compound L		
C(1)−N(1)	1.370(2)	C(4)−N(4)	1.371(2)
C(1)−N(2)	1.317(3)	C(11)−N(5)	1.331(2)
C(4)−N(3)	1.312(2)	C(7)−N(5)	1.331(2)
N(1)−C(1)−N(2)	111.11(17)	N(3)−C(4)−N(4)	112.13(17)
C(7)−N(5)−C(11)	116.89(15)		
	Compound **1a**		
Zn(1)−Cl(1)	2.2367(7)	Zn(1)−N(3)	2.022(2)
Zn(1)−Cl(2)	2.2539(7)	Zn(1)−N(2A)[a]	2.0114(19)
Cl(1)−Zn(1)−Cl(2)	113.59(3)	Cl(2)−Zn(1)−N(3)	109.82(6)
Cl(1)−Zn(1)−N(2A)[a]	117.40(7)	Cl(2)−Zn(1)−N(2A)[a]	104.44(6)
Cl(1)−Zn(1)−N(3)	105.14(6)	N(3)−Zn(1)−N(2A)[a]	106.16(9)
	Compound **2a**		
Zn(1)−Br(1)	2.3855(4)	Zn(1)−N(3)	2.012(2)
Zn(1)−Br(2)	2.3749(4)	Zn(1)−N(2A)[a]	2.024(2)
Br(1)−Zn(1)−Br(2)	114.133(14)	Br(2)−Zn(1)−N(3)	115.56(7)
Br(1)−Zn(1)−N(2A)[a]	109.79(6)	Br(2)−Zn(1)−N(2A)[a]	105.22(6)
Br(1)−Zn(1)−N(3)	105.22(6)	N(3)−Zn(1)−N(2A)[a]	106.67(9)

[a] Symmetry operations: (**1a**) A, $2 - y$, $1 + x - y$, $0.33333 + z$; (**2a**) A, $-y$, $x - y$, $-0.33333 + z$.

Single-Crystal X-ray Diffraction Studies. Typically, a suitable crystal was mounted on a glass fiber with silicone grease and placed in the cold stream of a Bruker APEX II with graphite-monochromated Mo Kα radiation ($\lambda = 0.710\ 73$ Å) at 150(2) K. All structures were solved by direct methods using SHELXS-97 and refined by full-matrix least-squares methods against F^2 with SHELXL-97.[27] Tables of neutral atom scattering factors, f' and f'', and absorption coefficients are from a standard source.[28] All non-hydrogen atoms were refined with anisotropic displacement parameters. All hydrogen atoms were located but not refined. The hydrogen atoms on the water molecule in **1a**,**b** and **2a**,**b** were not located. Crystallographic data for **1**−**3** and L are listed in Table 1. Selected bond lengths and angles are listed in Tables 2 and 3. Crystallographic data (excluding structure factors) for the structures in this paper have been deposited with the Cambridge Crystallographic Data

(27) Sheldrick, G. M. *SHELXTL*, version 5.1; Bruker AXS Inc.: Madison, WI, 1998.
(28) Sutton, L. E. *Tables of Interatomic Distances and Configurations in Molecules and Ions*; Chemical Society Publications: London, U.K., 1965.

Table 3. Selected Bond Lengths (Å) and Angles (deg) for **3a,b**

Compound **3a**			
Zn(1)−Cl(1)	2.2421(4)	Zn(1)−N(2)	2.0215(12)
Zn(1)−Cl(2)	2.2371(4)	Zn(1)−N(3A)[a]	2.0210(12)
Cl(1)−Zn(1)−Cl(2)	115.814(16)	Cl(2)−Zn(1)−N(3A)[a]	110.49(4)
Cl(1)−Zn(1)−N(2)	105.09(3)	Cl(2)−Zn(1)−N(2)	105.09(3)
Cl(1)−Zn(1)−N(3A)[a]	110.85(4)	N(2)−Zn(1)−N(3A)[a]	104.75(5)
Compound **3b**			
Zn(1)−Cl(1)	2.2273(4)	Zn(1)−N(3)	2.0148(13)
Zn(1)−Cl(2)	2.2502(4)	Zn(1)−N(2A)[a]	2.0344(13)
Cl(1)−Zn(1)−Cl(2)	120.817(18)	Cl(2)−Zn(1)−N(2A)[a]	102.82(4)
Cl(1)−Zn(1)−N(3)	104.66(4)	Cl(2)−Zn(1)−N(3)	112.32(4)
Cl(1)−Zn(1)−N(2A)[a]	111.41(4)	N(3)−Zn(1)−N(2A)[a]	103.68(5)

[a] Symmetry operations: (**3a**) A, $0.5 + x$, $0.5 - y$, $-0.5 + z$; (**3b**) A, $-0.5 + x$, $0.5 - y$, $1 - z$.

Centre as supplementary publication nos. CCDC 623490−623495 (**3a**, L, **2a**, **2b**, **1a**, and **1b**) and 638234 (**3b**). Copies of the data can be obtained, free of charge, on application to CCDC, 12 Union Road, Cambridge, CB2 1EZ, U.K. [Fax: +44(0)-1223-336033. E-mail: deposit@ccdc.cam.ac.uk.]

Results and Discussion

Structural Analysis of L. The ligand 2,6-bis(imidazol-1-yl)pyridine (L) was described previously.[25,26] We prepared L with a slightly different procedure by a one-pot reaction between 1*H*-imidazole, potassium hydroxide as base, and 2,6-dibromopyridine, which, after column chromatography, produced a comparable 74% yield. Since the C−N bonds connecting the imidazole rings and the central pyridine unit in L are flexible, these allow subtle conformational adaptation of L for the self-assembly of unique supramolecular structures (vide infra). To have a better insight into the structural changes of L from free ligand to polymeric structures, we determined its solid-state structure by X-ray diffraction study. A thermal ellipsoid plot of L·H_2O is shown in Figure 1. The structure reveals a full molecule of L and a guest water molecule in the asymmetric unit. The incorporation of water molecules in the lattice is presumably due to the wet acetone solvent used in crystal growth. The two imidazole rings are in syn orientation with their hydrogen atoms upon NC*N* carbons pointing away from the pyridine nitrogen donor (i.e., conformation **I** in Scheme 1). The two imidazole rings are essentially coplanar with the central pyridine unit. The interplanar angles between the two imidazole rings and the central pyridine are 3.84(6) and 4.07(7)°, which are very similar to those of 3.3 and 3.6° in the closely related 2,6-bis(1′-triazolo)pyridine dihydrochloride.[25]

Structural Analyses of 1 and 2. A simple hydrothermal reaction between ZnX_2 and L in a Teflon-lined autoclave afforded straightforwardly, well-formed, colorless crystals of **1** (X = Cl) and **2** (X = Br) in 66 and 88% of yields, respectively. These crystalline solids are insoluble in common organic solvents. The IR spectra of **1** and **2** are similar to that of the free ligand. The weak absorption bands at 3527 and 3537 $cm^{-1}$are assignable to the OH stretching bands in **1** and **2**, respectively. For L, there is a single strong absorption at 1494 cm^{-1}, which is split into two signals at ca. 1505 and 1466 cm^{-1} in **1** and **2**. X-ray diffraction study on a randomly picked crystal from **1** was performed. The structure **1a** was solved in the chiral space group $P3_221$ with

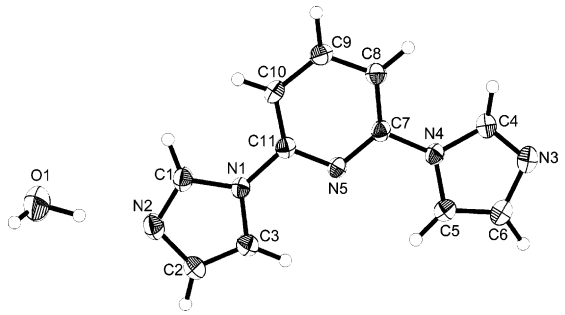

Figure 1. Molecular structure of L·H_2O with the thermal ellipsoids at 50% probability level. H atoms are of arbitrary size.

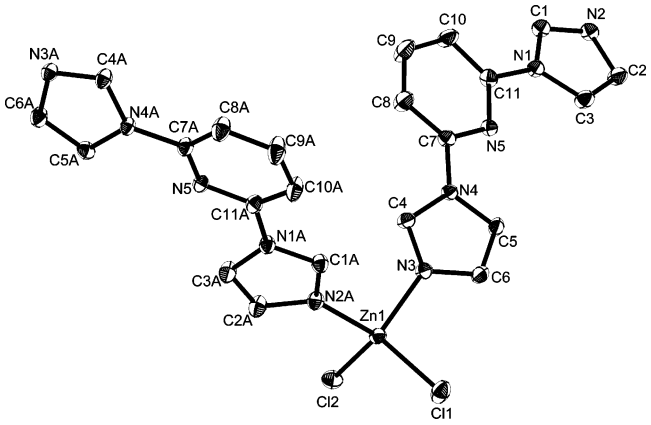

Figure 2. Molecular structure of **1a** showing the local coordination geometry. (The guest water molecule and hydrogen atoms were removed for clarity.) Thermal ellipsoids are shown at 50% probability level. H atoms are of arbitrary size. Symmetry code: (A) $2 - y$, $1 + x - y$, $0.33333 + z$.

an empirical formula of $ZnLCl_2 \cdot 0.5H_2O$ in the asymmetric unit. As depicted in Figure 2, the Zn(II) ion in **1a** adopts a slightly distorted tetrahedral coordination geometry with ∠Cl1−Zn1−N2A of 117.40(7)° deviated significantly from the ideal 109.5°. The ligand L is in conformation **I** with the pyridine N atom nonmetal-binding. It acts as a ditopic ligand via the imidazole N atoms bridging $ZnCl_2$ units, resulting in infinite 3_2 helices along the *c*-axis (Figure 3). All of these helices are left-handed (*M*-helices) with a large helical pitch of ca. 25.3 Å. The Flack parameter of −0.004(11) reflects the homochirality of the crystal.[29] The most intriguing feature is that the 3_2 helices are paired forming a unique double helical structure. Guest water molecules are present, linking the two strands via hydrogen bonding interactions (C···O = 3.319(7) and 3.648(5) Å) (see also Figure 1S in the Supporting Information). Pyridine rings on the two strands are stacked (offset face to face distance = 3.57 Å), contributing to the stability of the double helix. Notably, the two imidazole rings are rotated symmetrically along the C−N bonds making about the same interplanar angles (15.3 and 15.6°) with the central pyridine. This twisting is crucial to direct the Py and the NC*H*N protons toward the O atom of the water molecule for hydrogen-bonding interactions. If one

(29) For **1a** (*M*-helicity) refinement in space group $P3_221$ gave $R_1 = 0.0267$ ($I > 2\sigma(I)$) and Flack parameter = −0.004(11), whereas refinement in its enantiomorphic space group $P3_121$ gave $R_1 = 0.0504$ and Flack parameter 1.006(21).

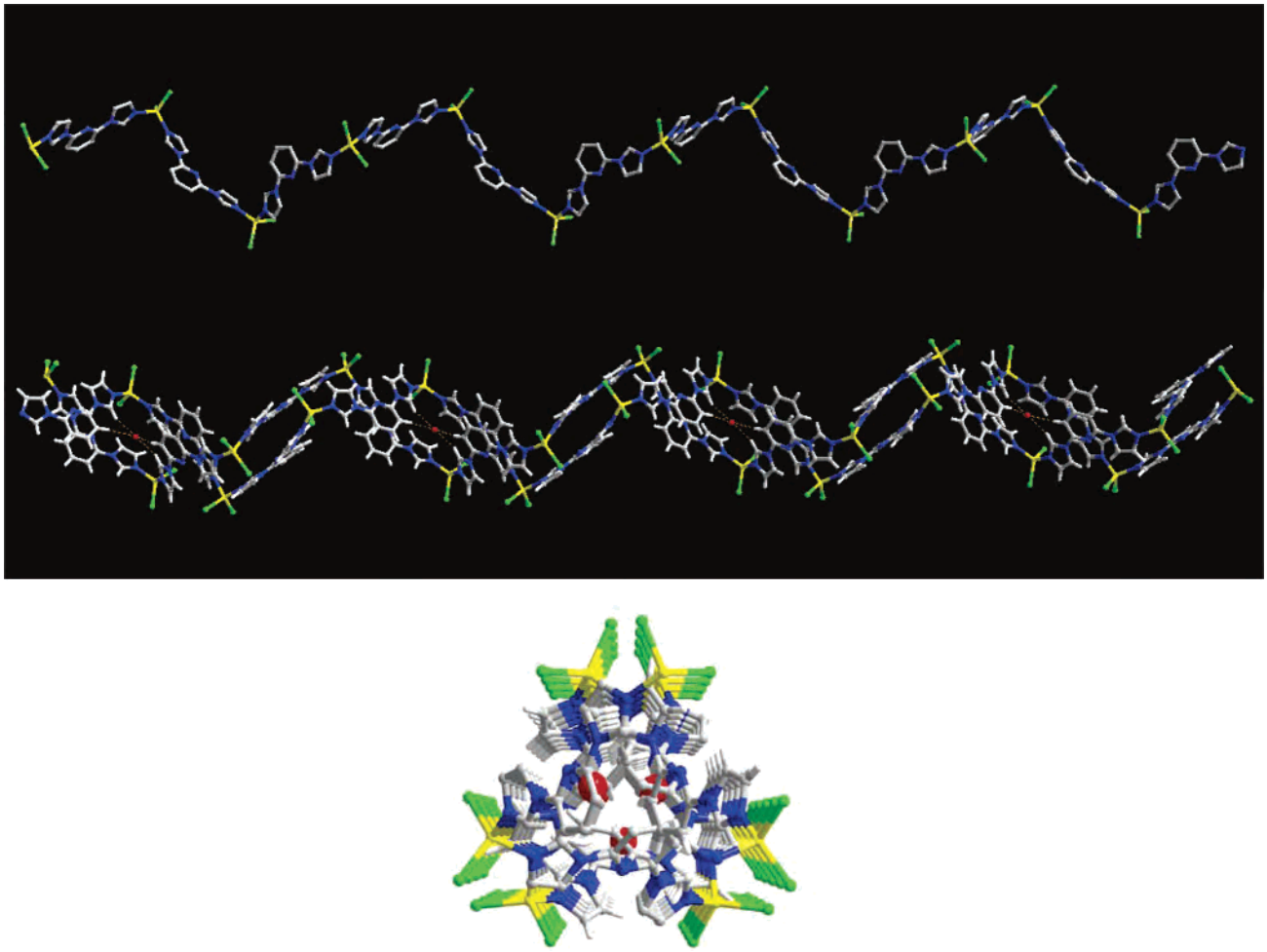

Figure 3. Top: Portion of the infinite *M*-helix in **1a.** H atoms are omitted for clarity. Middle: Two 3_1 *M*-helices are paired forming the double helix. The CH···O hydrogen-bonding interactions are shown in broken lines. Bottom: 3_1 double helices along the axis direction (*c*-axis). Color codes: green, Cl; blue, N; red, O; gray, C; white, H; yellow, Zn.

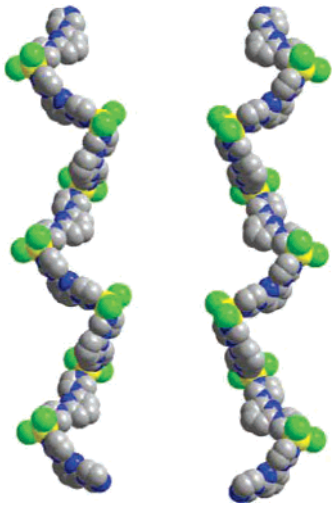

Figure 4. Portions of the infinite *M*- and *P*-helices in **1a** (left) and **1b** (right).

takes into account that the corresponding angles in the free ligands are just 3.84(6) and 4.07(7)°, the twisting is indeed significant.

The peripheral of each double helix is decorated with $ZnCl_2$ units. The two Cl atoms on each $ZnCl_2$ unit are

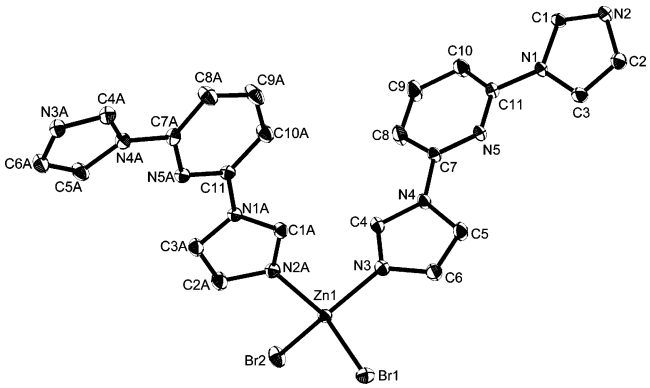

Figure 5. Molecular structure of **2a** showing the local coordination geometry. (The guest water molecule and hydrogen atoms were removed for clarity.) Thermal ellipsoids are shown at 50% probability level. H atoms are of arbitrary size. Symmetry code: (A) $-y, x - y, -0.33333 + z$.

involved in hydrogen-bonding interactions with the imidazole and pyridyl H atoms and O atoms of the guest water molecules (C···Cl = 3.567−3.605 Å and O···Cl = 3.172 Å) interlocking the double helices laterally into a densely

(30) For **1b** (*P*-helicity) refinement in space group $P3_121$ gave $R_1 = 0.0229$ ($I > 2\sigma(I)$) and Flack parameter = 0.002(10), whereas refinement in its enantiomorphic space group $P3_221$ gave $R_1 = 0.0502$ and Flack parameter 0.997(21).

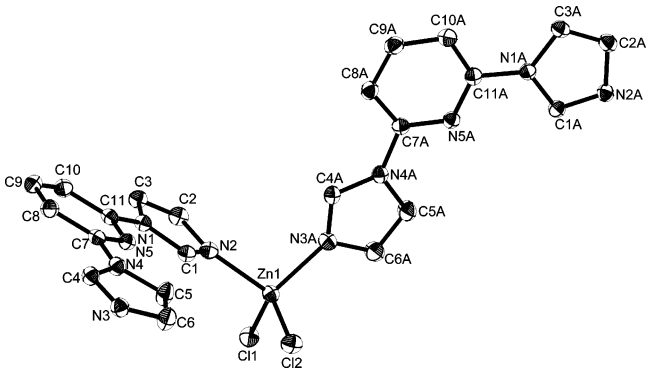

Figure 6. Molecular structure of **3a** showing the local coordination geometry (hydrogen atoms removed). Thermal ellipsoids are shown at the 50% probability level. Symmetry code: (A) $0.5 + x$, $0.5 - y$, $-0.5 + z$.

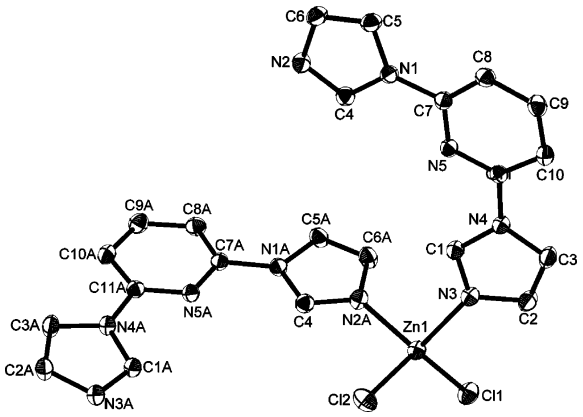

Figure 8. Molecular structure of **3b** showing the local coordination geometry (hydrogen atoms removed). Thermal ellipsoids are shown at the 50% probability level. Symmetry code: (A) $0.5 + x$, $0.5 - y$, $1 - z$.

packed homochiral 3D-coordination framework (see Figure 2S in the Supporting Information). It should be noted that the water molecules also take part in the lateral packing of the double helices, and all these hydrogen bond interactions should be responsible for the chirality preservation and spontaneous resolution when the helical chirality was extended into the homochiral 3D-network.

To unambiguously confirm the occurrence of spontaneous resolution in this system, we randomly picked another piece of crystal from the bulk sample **1** and performed a full structural characterization. The second crystal is of nondifferentiable habit from the first piece. The refinement of this second crystal in the same space group $P3_221$ and atomic coordinates resulted in a R_1 value of 0.0502 and a Flack parameter of 0.997(21), indicating a wrong absolute structure.[30] In fact, this structure **1b** is the enantiomer of **1a** and was packed in the enantiomorphic space group $P3_121$ instead.[30] The refinement in this space group achieved a Flack parameter of 0.002(10) and the structure comprises of 3_1 helices of right-handedness (*P*-helicity) (helical axes 3_1 and 3_2 are mirror images of each other) (Figure 4). The formation of a conglomerate is further confirmed albeit with a slightly higher ratio of **1a**:**1b** (7:3) determined by full structural refinement of totally ten independent, randomly picked crystals of the same sample.

The structures of **2a** (*M*-helicity) and **2b** (*P*-helicity) obtained from $ZnBr_2$ and L are isomorphic to those of **1a**,**b**. Figure 5 shows the coordination environment around the zinc center in **2a**. A significant different from **1** is that the asymmetric unit in **2** contains the empirical formula, $ZnLBr_2 \cdot 0.25H_2O$, indicating that only half of the water sites are occupied; also, rather interestingly, the enantiomorphic pair is visually distinguishable. Crystals of **2a** are of prismatic habit, whereas those of **2b** are hexahedrons. Crystals of **2a** or **2b** can be picked manually more than three times in a

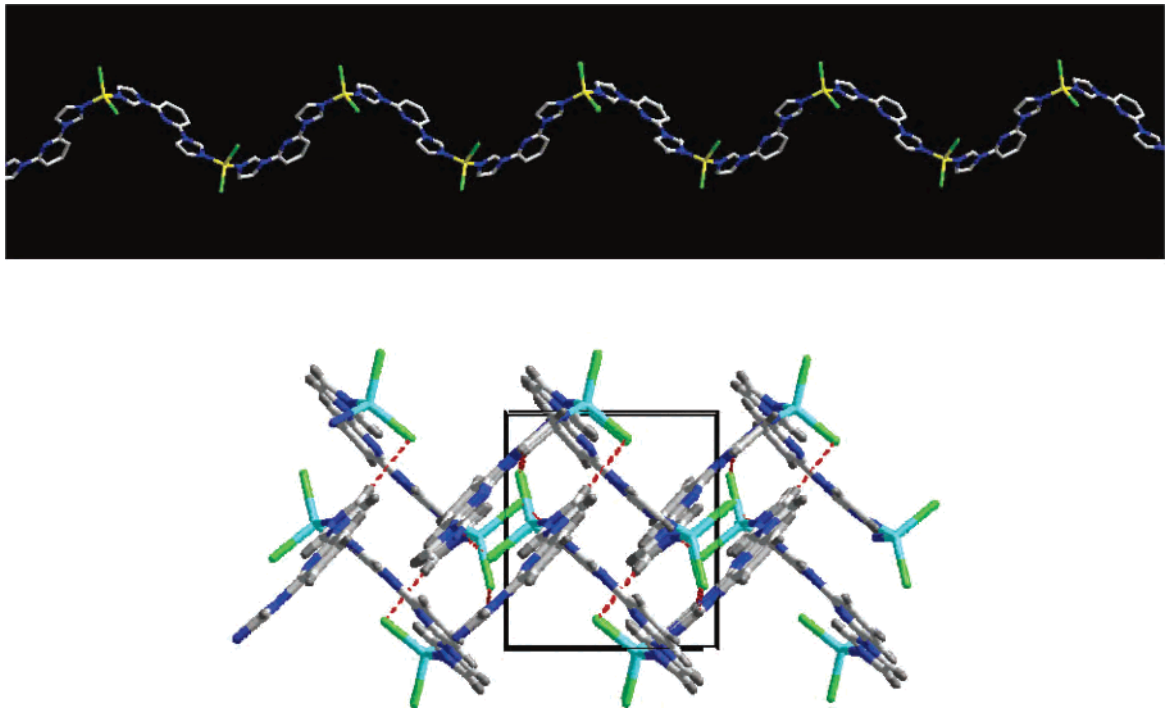

Figure 7. Above: Portion of the infinite zigzag chain in **3a.** Below: Perspective view along the *c*-axis showing the packing of chains in **3a.** The CH···Cl hydrogen-bonding interactions are shown in broken lines.

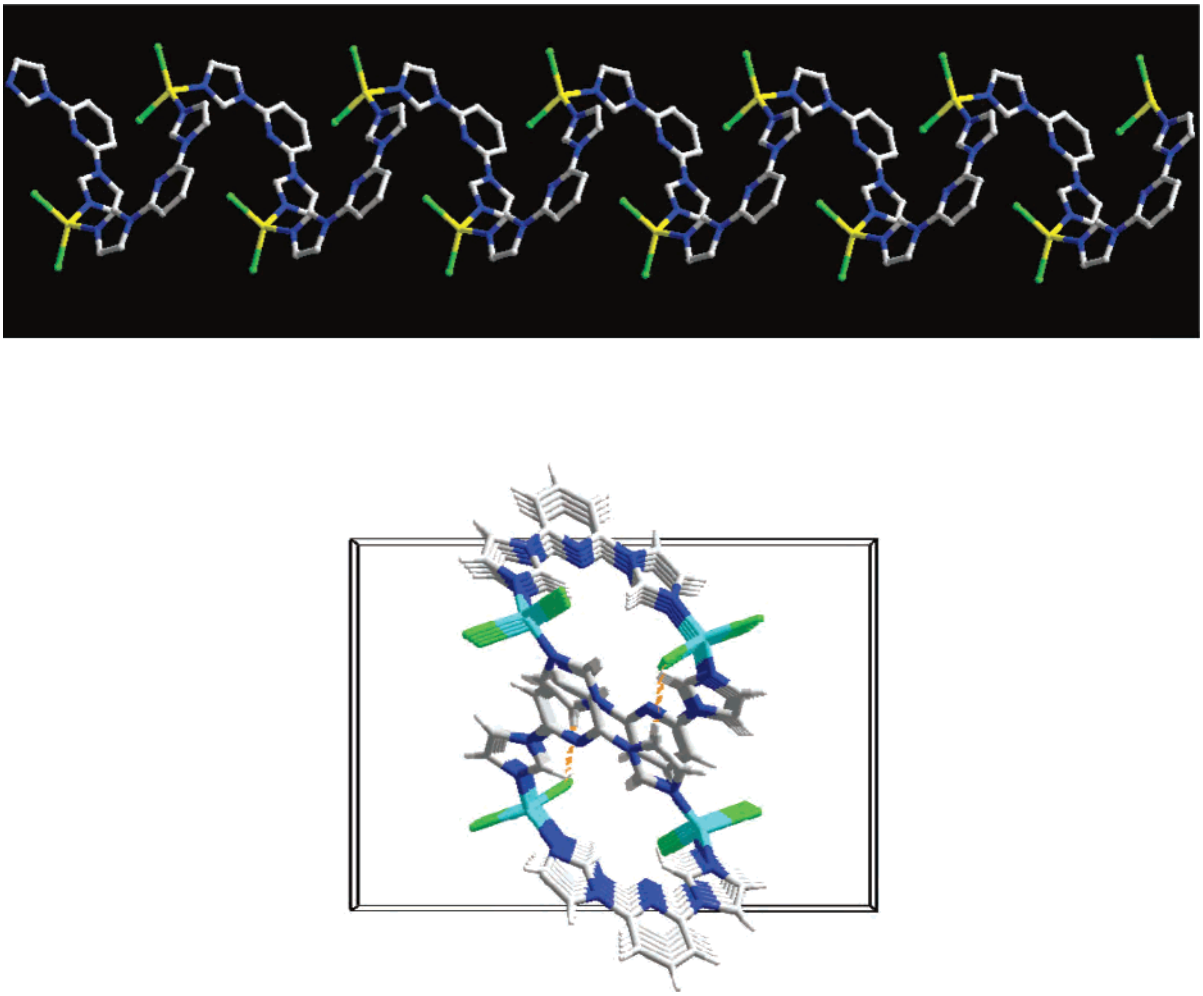

Figure 9. Above: Portion of the infinite 2_1 single helix in **3b.** Below: Perspective view along the *a*-axis showing two helices packed about a center of symmetry. The CH···Cl hydrogen-bonding interactions are shown in broken lines.

row with correct helicities confirmed by subsequent full structural determination.

Structural Analysis of 3a. To elucidate the importance of guest water molecules in the homochiral frameworks in **1**, we aimed at obtaining a guest-free complex between L and $ZnCl_2$. To ensure a moisture-free condition, we carried out a slightly different procedure from that of **1** and **2** for the preparation of the guest-free complex. Instead of using the Teflon-lined autoclave, we performed the solvothermal synthesis with $ZnCl_2$ and L in dried DMF, which were loaded in a scintillation vial inside a glovebox. The amount of crystalline product formed were then monitored visually. After heating of the sample for 30 h, appreciable amount of colorless crystals were formed, affording a yield of 55%. Like **1** and **2**, the crystalline solid is also insoluble in common organic solvents. Its IR spectrum is similar to that of **1** and **2**, with the OH stretching band at ca. 3530 cm^{-1} absent. Two separate signals at ca. 1500 and 1466 cm^{-1} are observed as well. In sharp contrast to **1** and **2**, $ZnLCl_2$ (**3a**) crystallizes in the achiral space group $P2_1/n$. Figure 6 depicts the coordination environment around the zinc center. Unlike **1** and **2**, the ligand L adopts the conformation **II** with the two imidazole moieties pointing in opposite direction. The two imidazole rings of L are rotated asymmetrically along the C−N bonds making significantly smaller interplanar angles of 5.2 and 8.2° with the central pyridine unit. A comparison of Figures 2 and 6 clearly shows that the relative orientations of the two ligands, due to the rotation of Zn−N bonds, on the zinc centers in **1a** and **3a** are different. In contrast to the helical polymeric structure in **1a**, the structure of **3a** consists of infinite zigzag chains of $ZnLCl_2$ along the [101] direction (Figure 7). Each of these chains are linked by extensive C−H···Cl hydrogen bonds involving the imidazole ring H and Cl atoms (C···Cl = 3.524−3.701 Å) into an achiral 3D-coordination network

Structural Analysis of 3b. Carrying out the solvothermal synthesis between $ZnCl_2$ and L in wet DMF under the same condition for **3a** afforded a mixture of crystals. Crystals of **1** were present as revealed by the unit cell measurement on a single crystal randomly picked from the bulk sample. We anticipated the presence of crystals of **3a** in the sample. Surprisingly, the unit cell measurement on a second crystal revealed a new cell parameters. A full structural analysis revealed a polymorph of **3a**. This genuine supramolecular isomer **3b** crystallized in the orthorhombic space group *Pbca*. Subsequent PXRD study also confirmed that the bulk sample is a mixture of **1** and **3b** (see Figure 3S in the Supporting Information). Figure 8 shows the coordination environment

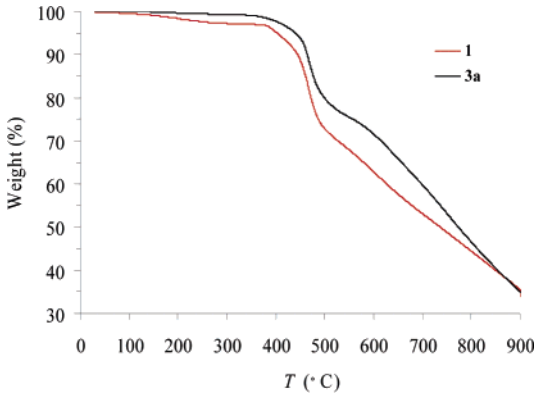

Figure 10. TGA curves of **1** and **3a** under nitrogen.

Scheme 2. Structural Relationship between 1D Chains and Conformations of L

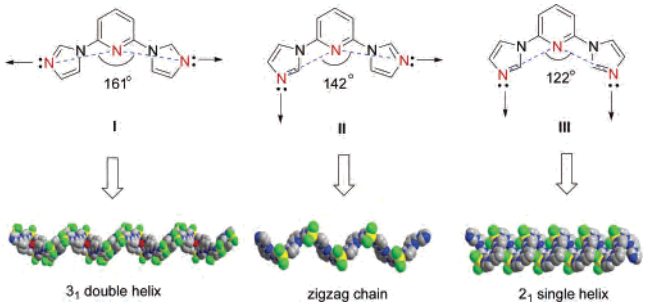

around the zinc metal. Unlike **1**, **2**, and **3a**, the ligand L is in conformation **III** with one of the imidazole rings almost coplanar with the central pyridine unit (interplanar angle = 4.57(4)°), whereas the other makes an interplanar angles of 12.10(5)°. The ditopic ligand L and $ZnCl_2$ units form an infinite 1D 2_1 helical chains propagating along the *a*-axis (Figure 9, top). The helical pitch of 9.45 Å is much smaller than that in **1a** (25.3 Å). Unlike **1** and **2**, **3b** is packed in a centrosymmetric unit cell and the helical chains are related by centers of symmetry (Figure 9, bottom). Thus, each crystal of **3b** is achiral. Like **3a**, hydrogen-bonding interactions involving H atoms on the imidazole rings and Cl atoms (C···Cl = 3.545−3.623 Å) are important in the 3D packing of the achiral solid.

Structural Aspect of L and 1D Chain. As shown in Scheme 1, the two donor imidazole N atoms in each of the three conformers of L enclose a different predetermined angle. To have a better insight of the conformational effect on the supramolecular motif, we quantified the enclose angles by measuring the N···N···N angles from their corresponding X-ray structures. As shown in Scheme 2, conformation **I** has the largest angle of 161°. The wide angle allows the formation of $3_1(3_2)$ helix with large pitch distance. Two of these helices are then winded together forming the double helix to achieve a dense packing. A ~20° smaller in the enclose angle favors the formation of zigzag chain, whereas the narrower angle of 122° led to 2_1 single helix with small pitch distance.

Thermal Properties. Thermogravimetric analysis (TGA) under nitrogen shows that the solid-state structures of **1** and **3a** are highly robust (Figure 10). For **1**, the gradual weigh loss of 2.59% (2.53% theoretically) in the range of 45−270 °C corresponds to the loss of the guest water molecule. Then it shows no weigh loss up to ca. 400 °C. For **3a**, there is no obvious weigh loss in the range of 45−400 °C, which is consistent with its guest-free nature.

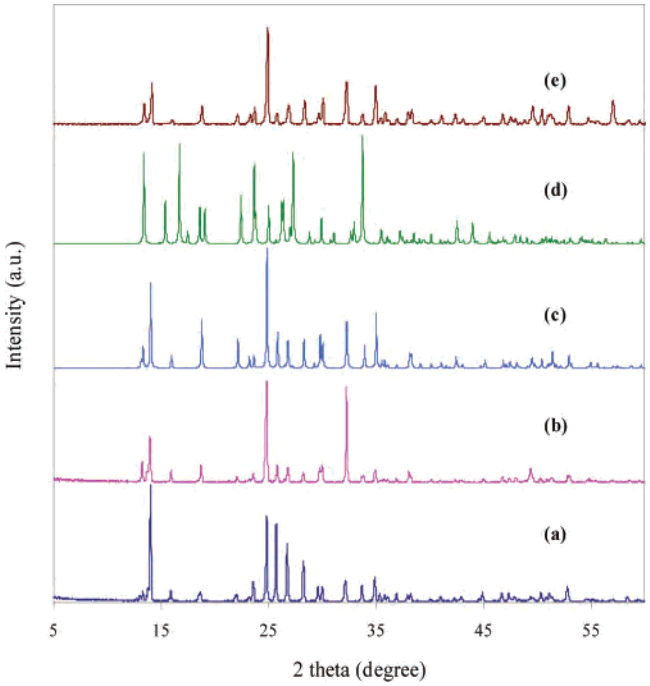

Figure 11. Powder XRD patterns: (a) **1** (conglomerate), as-synthesized; (b) **1** (conglomerate), after heat treatment; (c) simulation based on the single-crystal analysis of **1b**; (d) **3a**; (e) **3a** after heating in water (**3a** → **1**). Radiation: Fe Kα, λ = 1.937 28 Å.

Powder X-ray Diffraction and Structural Transformation. To gain insight into the dehydration phase of **1**, we carried out PXRD study on a sample of **1** which had been heated at 350 °C for 2 h. This dehydrated sample shows a PXRD pattern essentially identical with that of an authentic sample of **1**, reflecting that no phase transformation from **1** to **3a** or **3b** occurred upon dehydration and the framework of **1** remains intact even after removal of the guest water molecules (Figure 11). Next, it is necessary to check whether the reverse transformation from **3a** or **3b** to **1** is feasible. Thus, crystals of **3a** was allowed to suspend and stirred in water at 50 °C for 24 h. The material gradually lost its crystallinity and subsequent PXRD study on the powder indicated that **3a** was cleanly transformed to **1** (see Figure 11). Similar transformation was also observed by stirring the crystalline mixture of **1** and **3b** in water. PXRD study on the amorphous product shows the diffraction pattern of **1** remained (see Figure 3S in the Supporting Information). Consistently with the TGA result, stirring a suspension of crystalline sample of **1** in DMF at 50 °C for 24 h afforded an amorphous solid, which showed no change in its PXRD pattern.

It is worthy to compare **1** with the relevant system concerning helical structural motif reported by Aoyama and et al.[5] The solid-state structure of $L'Cd(NO_3)_3 \cdot H_2O \cdot EtOH$ (**A**), in which L′ is the achiral anthracene−pyrimidine derivative 5-(9-anthracenyl)pyrimidine, is also comprised of spontaneous resolved helical chains. A solvent effect is similarly in display. In the absence of ethanol, the achiral

L′Cd$(NO_3)_3$·$3H_2O$ (**B**) with zigzag chain structure was obtained. For this Cd/L′ system, the homochiral helical motif and achiral zigzag motif are interconvertible by introduction/removal of the guest ethanol molecules, exhibiting a kind of chirality memory effect.[5] A striking contrast for the Zn/L system is that the achiral **3a** or **3b** can be transformed readily to the homochiral framework of **1**, but not vice versa. The results suggest that **1** is thermodynamically more stable than **3a**,**b** and the guest water molecules function as template molecules. They are essential for inducing the initial double-helix formation and the assembly of the homochiral 3D-networks. Afterward, they can be eliminated with structural integrity retained. Nevertheless, the feasible transformation of the achiral **3a**,**b** to the homochiral motif of **1** suggests a chirality memory effect, similar to the Cd/L′ system.

Conclusions

In summary, we present a simple coordination system based on L and ZnX_2 which allows a certain degree of flexibility in C−N and Zn−N bond rotations. This preset flexibility is capable of transforming into 1D coordination polymers of diverse structures. In the presence of guest water molecules which provide the input of hydrogen-bonding interactions, rare spontaneous resolved double helices of Zn(II) coordination polymers **1** and **2** are successfully obtained. In dried DMF, **3a** with achiral networks of zigzag chains is formed instead. The polymorph **3b** featuring 2_1 single helical chains was obtained in wet DMF. In contrast to the relevant system showing similar solvent effect,[5] the framework of **1** is highly stable (up to 350 °C) and its homochiral integrity is maintained even after removal of the guest water molecules, which play a template role for the supramolecular assembly. In contrast, the reverse transformation from the achiral zigzag motif of **3a** or the 2_1 single helix motif of **3b** to the homochiral helical motif of **1** can take place, illustrating the thermodynamic stability of **1** and the importance of water in inducing its supramolecular structure. The high robustness and the stable homochiral framework associated with the present system are desirable characteristics for new functional crystalline materials.

Acknowledgment. This work was supported by the National Science Council of Taiwan.

Supporting Information Available: X-ray data in CIF format, packing diagrams of **1a**, and powder XRD patterns of **3b**. This material is available free of charge via the Internet at http://pubs.acs.org.

IC700428E